JOURNAL OF VIROLOGY, Mar. 1986, p. 1073–1083
0022-538X/86/031073-11$02.00/0

Vol. 57, No. 3

Transforming Sloan-Kettering Viruses Generated from the Cloned v-*ski* Oncogene by In Vitro and In Vivo Recombinations

EDWARD STAVNEZER,[1]†* ALEXANDER E. BARKAS,[2]‡ LYNN A. BRENNAN,[1] DAVID BRODEUR,[1] AND YEN LI[1]§

Molecular Biology and Virology Unit, Graduate School of Medical Sciences, Memorial Sloan-Kettering Cancer Center, New York, New York 10021,[1] and Biology Department, New York University, New York, New York 10012[2]

Received 9 July 1985/Accepted 19 November 1985

The Sloan-Kettering viruses (SKVs) are replication-defective retroviruses that transform avian cells in vitro. Each of the three SKV isolates is a mixture of viruses with genomes ranging in size from 4.1 to 8.9 kilobases (kb) with a predominant genome of 5.7 kb. Using a cDNA representing a sequence, v-*ski*, that is SKV specific and held in common by the multiple SKV genomes, we generated a restriction map of the 5.7-kb SKV genome and molecularly cloned a *ski*-containing fragment from SKV proviral DNA. Southern hybridization and sequence analysis showed that the cloned DNA fragment consisted of the 1.3-kb *ski* sequence embedded in the p19^{gag} sequence and followed by the remaining 5′ half of the *gag* gene and small portions of both the *pol* and *env* genes. A large deletion encompassing the 3′ half of *gag* and the 5′ 80% of *pol* was mapped to a position about 1 kb downstream from the 3′ *ski-gag* junction. To determine whether the cloned *ski* sequence had transforming activity, the *ski*-containing fragment and a cloned Rous-associated virus 1 (RAV-1) genome were used to construct an analog of the 5.7-kb SKV genome, RAV-SKV. Cotransfection of chicken embryo cells with RAV-SKV and RAV-1 yielded foci of transformed cells whose morphology was identical to that induced by the natural SKVs. The transformed transfected cells produced transforming virus with a 5.7-kb *ski*-containing genome and synthesized a *gag*-containing polyprotein of 110 kilodaltons (kDa). Several nonproducer clones of RAV-SKV-transformed cells were analyzed, and most were found to synthesize a 5.7-kb SKV RNA and a 110-kDa polyprotein. One clone was found to contain an 8.9-kb SKV RNA, and this clone synthesized a 125-kDa polyprotein. Since both the 5.7- and 8.9-kb genomes and the 110- and 125-kDa polyproteins had been identified in studies on the natural SKVs, the present results not only demonstrate the transforming activity of these individual SKVs but also suggest mechanisms for their generation.

The Sloan-Kettering viruses (SKVs) are acute transforming retroviruses that were isolated from cultured chicken embryo cells (CECs) (26). By preparing an SKV-specific cDNA we found that all of the SKV genomes share a specific sequence, *ski*, which is closely related to a sequence in chicken DNA, c-*ski* (16). Chicken c-*ski* was shown to have homologs in the genomes of distantly related species and to be transcribed into poly(A)-containing RNA in uninfected chicken cells (16). These properties of *ski* are shared by the cell-derived oncogenes of all acute transforming retroviruses (4, 5).

The oncogene-like properties of *ski* did not, however, directly establish its role in SKV-induced cellular transformation. Our cDNA studies did not show whether *ski* represented only a single continuous sequence derived from a single cellular gene. We had identified two novel *gag*-containing polyproteins, p110 and p125, in SKV-transformed cells, but we did not determine which SKV genome(s) encoded these proteins or whether either or both proteins contained amino acid sequences encoded by *ski*. The present report details the studies we performed to address these unknowns. Using restriction mapping, molecular cloning, and in vitro recombination to generate an SKV analog (Rous-associated virus [RAV]-SKV), we positively identified *ski* as the SKV oncogene and showed that it is expressed by different SKV genomes in either the p110 or p125 form.

Our earlier studies showed that each of the three natural SKV isolates comprised a heterogeneous mixture of *ski*-containing genomes, ranging in size from 4.1 to 8.9 kilobases (kb) (16, 26). It seemed likely that this multiplicity was the result of a nonrandom set of deletion events (7). We had noted that the ratio of genome sizes remained relatively stable during multiple virus passages (26); this observation did not appear to be consistent with an ongoing process of deletion formation. In the present study we found that, starting with a molecular clone of RAV-SKV (5.7 kb), a new SKV genome (8.9 kb) was generated upon transfection and subsequent virus spread. On the basis of our analyses of the sequence organization of both the molecular clone and the 8.9-kb genome, we present a model involving SKV-avian leukosis virus (ALV) recombination which explains this observation and may account for both the generation and preservation of the multiple SKV genomes.

MATERIALS AND METHODS

Cells and viruses. Primary CECs were prepared and cultured as described previously (26) from embryonated eggs of line 0 (ev$^-$) (1), possessing no endogenous viral loci (Regional Poultry Research Laboratory, East Lansing, Mich.) or line 11, possessing ev1 and ev4 (SPAFAS, Inc., Norwich, Conn.) (1). Cultures of quail embryo cells (QECs) were prepared from embryonated eggs of random-bred Japanese quails essentially as described for CECs.

* Corresponding author.
† Present address: Department of Biochemistry and Molecular Biology, University of Cincinnati Medical Center, Cincinnati, OH 45267-0522.
‡ Present address: Whitehead Institute for Medical Research, Cambridge, MA 02139.
§ Present address: Center for Cancer Research and Department of Biology, Massachusetts Institute of Technology, Cambridge, MA 02139.

The viruses employed were: transformation-defective Bratislava 77 (tdB77; from P. K. Vogt), SKV770 (26), SKV785.7 E1 (16), and SKV780 B12 (a biologically cloned derivative of SKV780 containing a single 5.2-kb SKV genome and the helper virus, tdB77) (see Results).

Preparation of cDNA. Employing 6 to 15 μg of 50S to 70S RNA from SKV770 as template, a ^{32}P-labeled representative cDNA was synthesized and purified as previously described (26). The fraction of cDNA representing SKV-specific sequences ($cDNA_{SKV}$; 6 to 9%) was selected by its inability to hybridize with a vast excess of viral RNA from transformation-defective Rous sarcoma virus (RSV), Prague strain, subgroup B, Prague strain, subgroup C RSV (PrC RSV), or tdB77 (16).

Isolation of RNA and DNA. Viral 50S to 70S RNAs were isolated from pelleted viruses as previously described (16, 26). Cytoplasmic poly(A)$^+$ RNA was prepared as described by Weiss et al. (32). Genomic DNAs were prepared from nuclei (32) of cultured CECs and QECs by sodium dodecyl sulfate (SDS)-pronase treatment and organic extraction (14). Bacteriophage and plasmid DNAs were purified by published procedures (19).

Electrophoresis and blotting of RNA and DNA. RNA samples were reacted with glyoxal and fractionated on 1% agarose gels (21) and transferred to nitrocellulose filters by the procedure of Thomas (29). Digestions of DNAs with restriction endonucleases were performed as recommended by the supplier and monitored for completeness (14). Digested DNAs (10 μg of genomic DNA or 0.2 to 1.0 μg of phage and plasmid DNA) were fractionated by electrophoresis on agarose gels and detected by ethidium bromide fluorescence followed by hybridization either in situ to dried gels (22) or after transfer to nitrocellulose membranes by a modified Southern procedure (25).

Blots were prehybridized and then hybridized at 42°C with cDNA or nick-translated DNA (23) probes in 50% (vol/vol) formamide–3× SSC (1× SSC is 0.15 M NaCl plus 0.015 M sodium citrate–Denhardt solution (10)–100 μg of sheared and denatured *Escherichia coli* DNA per ml–200 μg of yeast RNA per ml–50 mM sodium phosphate (pH 6.8)–10 mM EDTA. Blots were washed in 2× SSC–0.1% SDS at both room temperature and 50°C and in 0.1× SSC–1% SDS at 50°C.

Labeling and detection of viral proteins. Labeling of virus-infected and control uninfected cells with [^{35}S]methionine, preparation of lysates, immunoprecipitation, SDS-polyacrylamide gel electrophoresis (PAGE), and fluorography were performed as previously described (26). The antiserum employed was a rabbit anti-avian myeloblastosis virus *gag* serum prepared and generously provided by E. Fleissner (12). Exact conditions of labeling and analysis are given in the figure legends.

Plasmids and phage. An infectious, nonpermuted clone (pRAV-10R) of the genome of the ALV RAV-1 was obtained from J. M. Bishop. A defective permuted clone (pTD-1) of the genome of the ALV tdB77 was obtained from P. Shank. A *gag*-specific (*Sst*I to *Eco*RI) subclone (pB5gag) and a *pol*-specific (*Eco*RI to *Kpn*I) subclone of a partial RSV, Prague strain, subgroup A genome were described previously (26). A fragment from the 5′ end of the SR-A RSV clone pSRA-2 (9) from the *Eco*RI site in U3 of the long terminal repeat to the *Pvu*II site in the *gag* p19 sequence was subcloned between those restriction sites in pBR322 to yield the clone p5′NCR (unpublished data). Plasmid transformation, propagation, and purification with *E. coli* K-12 strain HB101 were performed by established procedures (19). The

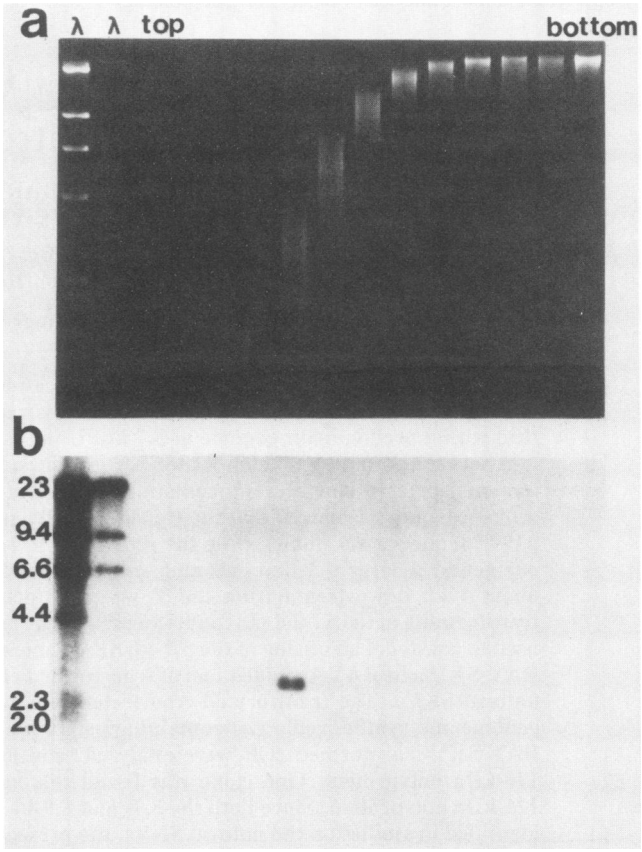

FIG. 1. Sucrose gradient purification of the 2.8-kb *Xho*I fragment containing v-*ski*. Genomic DNA from SKV770-infected CECs was digested to completion with *Xho*I and fractionated by velocity sedimentation through a 10 to 40% sucrose gradient as described in Materials and Methods. The gradient was collected from the top, and odd-numbered fractions were analyzed by agarose gel (0.7%) electrophoresis. Total DNA was visualized by ethidium bromide fluorescence (a), and *ski*-containing fragments were detected by in situ gel hybridization (b) with *ski*-specific cDNA (16). Molecular weight markers of lambda phage DNA digested with *Hin*dIII (sizes in kilobases given in panel b) were run in the two leftmost lanes and were detected in panel b by including nick-translated lambda DNA in the hybridization mixture.

lambda phage cloning vector L47.1 (18) was propagated on *E. coli* K-12 strain K803 (19). Phage were purified by isopycnic centrifugation, and phage DNA was prepared from DNase I-treated phage by SDS treatment and phenol-chloroform extraction.

Construction and screening of a partial library from SKV770-infected CECs. About 500 μg of genomic DNA from SKV770-infected SPAFAS line 11 cells was digested to completion with *Xho*I. The digested DNA was fractionated by rate-zonal sedimentation through a 10 to 40% (wt/vol) sucrose gradient in 1 M NaCl–10 mM Tris hydrochloride (pH 7.5)–1mM EDTA–0.2% SDS at 20°C and 25,000 rpm in a Beckman SW27 rotor for 18 h (19). The gradient was fractionated from the top (~1.5 ml per fraction), and the DNA in each fraction was quantitated by measuring the A_{260} and collected by ethanol precipitation. A portion of each odd-numbered fraction was analyzed by agarose gel electrophoresis followed by in situ gel hybridization with SKV-specific cDNA. The fractions constituting the major *ski*-containing fragments (2.8 ± 0.5 kb) were pooled and ligated

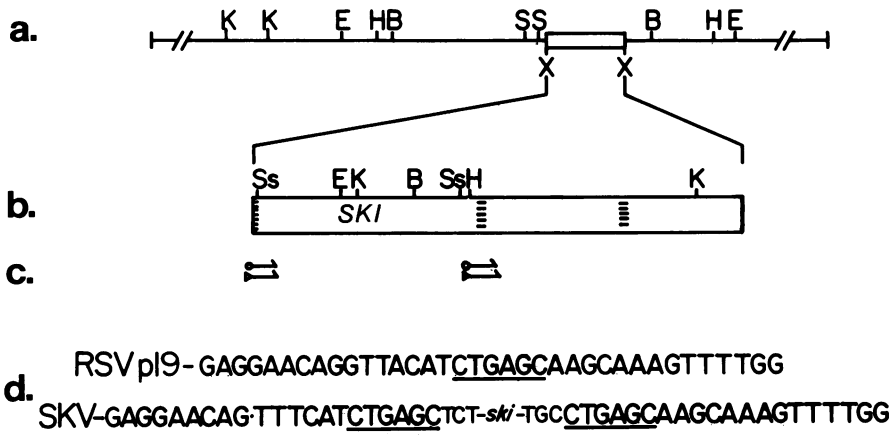

FIG. 2. Structure of v-*ski*-containing fragments in recombinant phages v-*ski*1 and v-*ski*5. v-*ski*-containing recombinant phage were obtained by cloning the gradient-purified DNA shown in Fig. 1. Two of the recombinants containing inserts that hybridized with both ALV and *ski* probes were mapped by restriction enzyme digestion and in situ gel hybridization with probes representing the *gag* and *pol* genes of ALV as described in Materials and Methods. The position and orientation of sites within the cloned segment (open box in part a and expanded in part b) were determined relative to their known locations in L47.1 (solid line in part a) with each of the enzymes shown both singly and in double digestions with *Sal*I. Part c shows the location of the *Xho*I and *Hin*dIII restriction sites used to generate both 5′ (○→) and 3′ (▷→) end-labeled fragments of each of the regions indicated that were subjected to Maxam-Gilbert sequence analysis. Part d gives the published sequence (24, 27) of a portion of the RSV p19 gene and part of the sequence from the ALV-*ski* junctions indicated in part c. The sequences are those of the viral or positive strands. Enzymes employed: B, *Bam*HI; E, *Eco*RI; H, *Hin*dIII; K, *Kpn*I; S, *Sal*I; Ss, *Sst*I; X, *Xho*I.

to an equimolar quantity of *cos* end-ligated, *Xho*I-digested L47.1 DNA. The ligated DNA was packaged into phage particles which were titrated and screened by hybridizing resulting plaque-lifts (3) with nick-translated pTD-1 and $cDNA_{SKV}$. Of the 80,000 plaques screened, 4 were positive and 2, lambda v-*ski*1 and lambda v-*ski*5, were picked and grown up for further analysis.

Transfection. Transfections of CECs were performed essentially as described by Corsaro and Pearson (8). Secondary CECs were seeded at 10^6 cells per 100-mm dish, fed after 24 h, and treated with DNA-calcium phosphate coprecipitates 4 h later. Precipitates of cloned DNAs were made in the presence of carrier DNA from uninfected line 0 (ev^-) CECs which was sheared to about 20 kb by repeated passage through a 26-gauge needle. Each plate received the precipitate formed with 20 μg of carrier DNA and 80 ng of pRAV-10R DNA, plus or minus 400 ng of RAV-SKV DNA. At 12 to 16 h after DNA addition, cells were washed twice with saline or medium, refed normal medium containing Polybrene (20 μg/ml), and incubated for 24 to 48 h. At this time and at subsequent passages when cells reached confluence they were split 1:4. Confluent cultures were monitored visually for the appearance of transformed foci.

DNA sequence analysis. DNA fragments were labeled at their 5′ termini with polynucleotide kinase and [γ-^{32}P]ATP or at their 3′ termini with phage T4 DNA polymerase and the appropriate [α-^{32}P]deoxynucleoside triphosphate. Labeling and subsequent sequence analysis were performed by the method of Maxam and Gilbert (20).

RESULTS

Cloning of a subgenomic, *ski*-containing fragment of the 5.7-kb SKV770 provirus. We employed both an SKV-specific probe ($cDNA_{SKV}$) and ALV cDNA to generate a crude restriction site map of the major provirus (5.7 kb) of SKV770 (data not shown). The main feature of this map was the positioning of the *ski* sequence in the *gag-pol* region of the genome, apparently at the site of a large deletion of viral sequences encompassing the 3′ half of *gag* and the 5′ 80% of *pol*. This conclusion was consistent with a Northern blot analysis of SKV770 RNAs with a set of probes from specific regions of the ALV genome that showed that the 5.7-kb genome did not contain sequences from the 5′ half of the *pol* gene (data not shown).

The mapping data identified a restriction fragment produced by cleavage with *Xho*I at sites in *gag* and *env* that seemed an ideal candidate for molecular cloning of the *ski* gene. The fragment was small (2.8 kb) relative to the average size of fragments of *Xho*I-digested chicken DNA (about 15 kb), allowing for significant purification by size selection. It was the only v-*ski*-containing *Xho*I fragment detected, and it encompassed the region of helper sequence deletion.

To clone the v-*ski*-containing fragment, we subjected genomic DNA from SKV770-transformed CECs to complete digestion with *Xho*I and fractionated the digestion products by sedimentation through a sucrose gradient. Samples of the gradient fractions were analyzed by electrophoresis and subsequent in situ gel hybridization with $cDNA_{SKV}$ (Fig. 1). The fractions containing the 2.8-kb v-*ski* fragment were pooled and ligated to *Xho*I-cut lambda L47.1 DNA. Phage plaques resulting from infection with the packaged DNA were screened by hybridization with both an ALV probe and $cDNA_{SKV}$.

Two of the positive plaques were grown up and analyzed by restriction mapping (Fig. 2a and b). They were found to be identical with respect to the position of all sites shown in Fig. 2. Subsequent mapping has revealed that v-*ski*1 and v-*ski*5 share 11 of 12 six-base restriction sites, differing only in a *Pvu*II site which is present in v-*ski*5 and absent in v-*ski*1. The results shown in Fig. 2a confirmed the presence of all of the restriction sites we had previously mapped in *ski* and allowed us to construct a more precise map of the *ski* region (Fig. 2b). However, in situ gel hybridization of restricted DNA to *gag*-specific and *pol*-specific probes yielded results that were not consistent with our earlier data. We had positioned *ski* at the site of a 3′ *gag* to 5′ *pol* deletion, leading us to expect that *ski* would be flanked by the remaining *gag*

sequence on its 5′ side and by the remaining *pol* sequences on its 3′ side. Contrary to our expectations we did not detect any *gag* sequences between the 5′ *Xho*I site and the 5′ end of *ski* (data not shown). These results indicated that the 5′-proximal *Xho*I site was derived either from the viral *gag* sequence but positioned very close to the 5′ end of *ski* or from the *ski* sequence itself. All of the fragments extending from restriction sites within *ski* to the 3′ *Xho*I site hybridized to both the *gag* and the *pol* probes. This result shows that the *ski* sequence is flanked by *gag* gene sequences at its 3′ end, suggesting that the large *gag-pol* deletion in the 5.7-kb genome occurred at an independent site from that of *gag-ski* recombination.

Nucleotide sequence at ALV-*ski* boundaries. The strategy we developed to clone *ski* intact was based on mapping data that positioned *ski* well within *Xho*I sites present in the *gag* and *env* sequences derived from tdB77. However, the results described above showing no hybridizable *gag* sequences between the 5′ *Xho*I site and the 5′ end of *ski* suggested the possibility that this *Xho*I site resided within the *ski* sequence. To resolve this issue before attempting to construct an SKV provirus, we sequenced the region extending from the 5′-proximal *Xho*I site into *ski* (Fig. 2c). To determine the position of the 3′ *ski*-tdB77 junction with respect to the large deletion, we also sequenced the region extending in the 3′ direction from the *Hin*dIII site in *ski* (Fig. 2c).

Comparing our sequence with the published sequences of SR-A RSV (27) and PrC-RSV (24), we found that, proceeding downstream from the 5′ *Xho*I site, the first 19 bases in our sequence were nearly identical to the RSV sequences extending in the 3′ direction from the *Xho*I site in *gag*-p19 (Fig. 2d). Beyond this short region of near identity the RSV and SKV sequences diverged. At the 3′ end of *ski* we found that the first 90 bases extending in the 3′ direction from the *Hin*dIII site were unrelated to the RSV sequence. The remainder of the sequence was identical to the RSV *gag* sequence starting with a repeat of the hexanucleotide CTGAGC that was found at the position where the RSV and SKV sequences had diverged at the 5′ end of *ski* (Fig. 2d). The results showed that no ALV sequences were deleted at the site of *ski* insertion. In fact, the hexanucleotide CTGAGC which formed a direct repeat at the boundaries of *ski* occurred only once at that position in the uninterrupted RSV-p19 sequence. The fact that *ski* was flanked by *gag*-p19 sequences at both ends confirmed our suggestion that the large deletion encompassing the 3′ half of *gag* and the 5′ 80% of *pol* occurred at an independent site from that of *gag-ski* recombination. Additional restriction mapping of the cloned fragment (data not shown) positioned the 5′ end of the deletion at least 700 bases downstream from *ski* in the p27 gene between bases 1356 and 1630 and the 3′ end in the *pol* gene between bases 4625 and 4995 (base numbers derived from the PrC-RSV DNA sequence of Schwartz et al. [24]).

Construction and analysis of RAV-SKV. Having found that the 5′ *Xho*I site in the cloned SKV fragment originated from the *gag*-p19 sequence, we constructed analogs of the 5.7-kb SKV provirus with the *Xho*I fragments from the two SKV-derived phage clones (Fig. 3). Three of the resulting RAV-1-SKV recombinants that contained the *Xho*I fragments in the correct orientation were separately cotransfected with RAV-1 DNA into CECs. By the second cell passage after transfection, multiple foci of epithelioid cells, typical of SKV-transformed CECs, appeared in cultures transfected with RAV-SKV5 plus RAV-1. No foci were seen in cultures transfected with either RAV-SKV1 plus RAV-1 or RAV-1 alone.

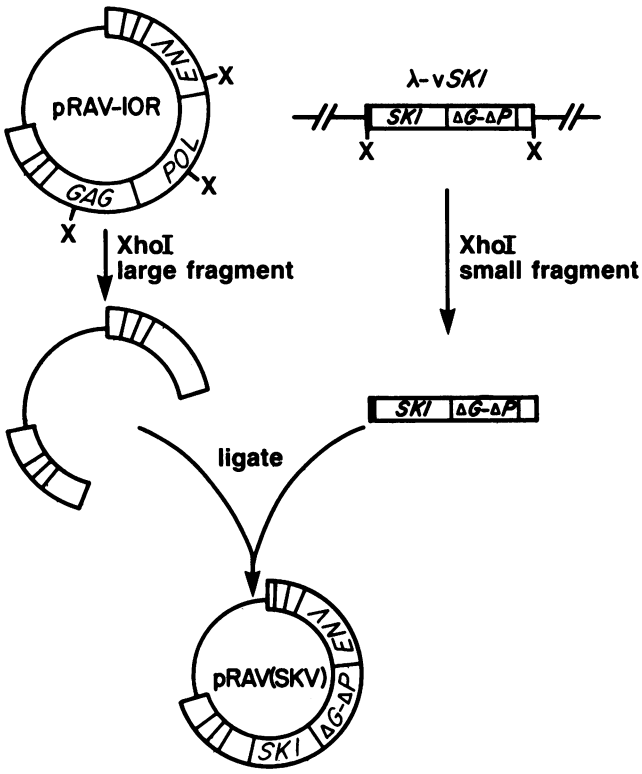

FIG. 3. Strategy for generating the recombinant virus RAV-SKV. A molecular clone (pRAV-10R) containing an infectious, nonpermuted copy of the genome of RAV-1 was digested with *Xho*I to delete the sequences between the sites in the *gag* p19 gene and the *env* gene. The 2.8-kb v-*ski*-containing *Xho*I fragments were isolated from the recombinant phages v-*ski*1 and v-*ski*5 by electroelution from agarose gels. The *ski*-containing fragments were separately ligated to the deleted RAV-1 DNA and cloned. Plasmids of the predicted size were purified and mapped by restriction enzyme digestion and gel electrophoresis to obtain recombinant genomes with the proper polarity. The initial screen yielded two such genomes with the insert from v-*ski*1 (1a and 1b) and one from v-*ski*5. ΔG-ΔP, *gag-pol* deletion.

After two additional cell passages all cells in the RAV-SKV5 cultures displayed the typical SKV-transformed phenotype. At this passage virus was harvested from all cultures to assay for transforming ability and to analyze viral RNAs. Only the virus harvested from the cultures transfected with RAV-SKV5 induced foci in monolayer cultures of CECs and transformed CECs to anchorage-independent growth in soft agar medium (data not shown). Viral RNAs produced by the transfected cells were analyzed by Northern blotting and hybridization with both ALV and *ski* probes (Fig. 4). The results showed that all of the transfected cultures produced virus with a 7.6-kb genome which hybridized only with the ALV probe; this RNA species is the genome of RAV-1. The virus produced by RAV-SKV5-transfected cells contained an additional RNA species of 5.7 kb that hybridized with both probes. Cells cotransfected with RAV-1 and either RAV-SKV1a or RAV-SKV1b failed to produce virus with a *ski*-containing genome (Fig. 4) and were phenotypically normal. We did not investigate the defect(s) in the constructs derived from v-*ski*1, but since they failed to yield infectious viruses, unless otherwise indicated, we refer to the virus derived from the v-*ski*5 construct as RAV-SKV.

Virus-encoded proteins in the transfected cells were ana-

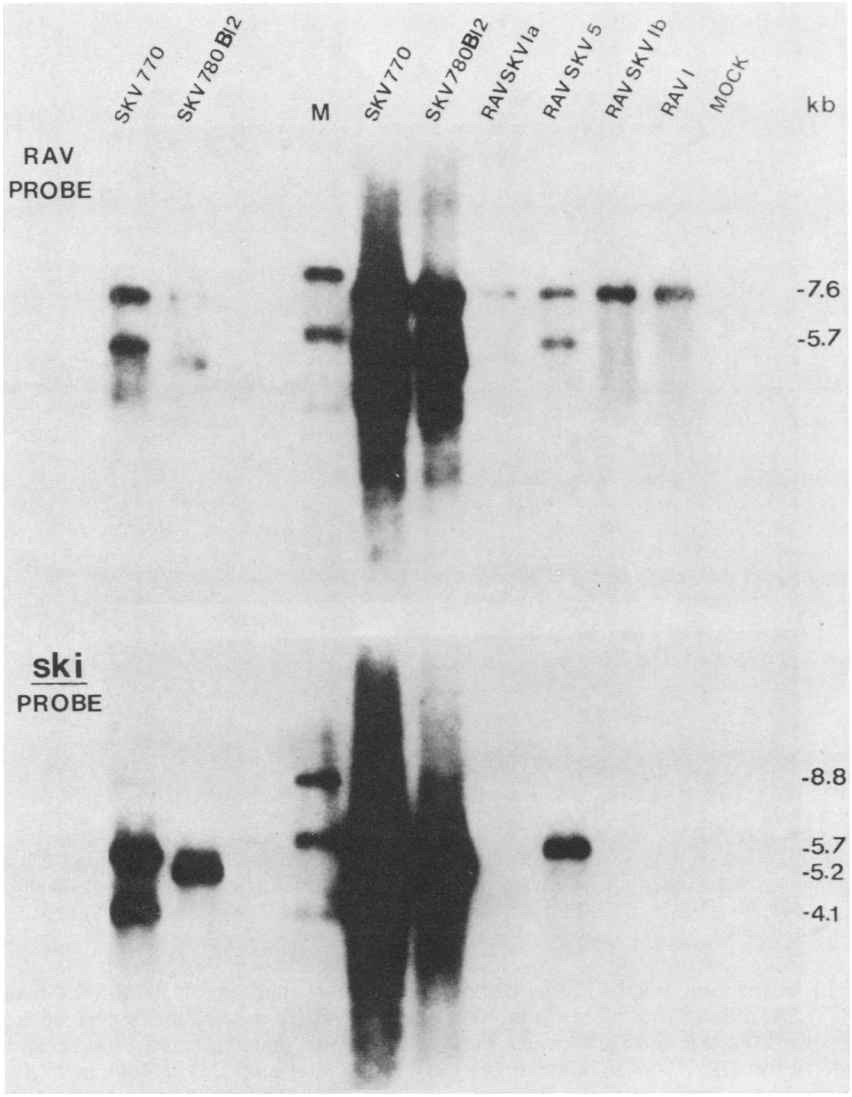

FIG. 4. Northern blot analysis of viral RNAs produced by cells transfected with RAV-SKV DNAs. CECs were subcultured four times after transfection with pRAV-10R DNA only or after cotransfection with pRAV-10R and each of the three RAV-SKV constructs (see the legend to Fig. 3). Control cultures received only carrier DNA (mock). Viral RNAs were purifed from 10 ml of medium containing virus produced by these cells and from control SKV-infected CECs during a 4-h interval as described in Materials and Methods. A Northern blot of these RNAs was hybridized with nick-translated pRAV-10R (upper panel). This probe hybridization was denatured, and the blot was hybridized with a *ski*-specific probe (the plasmid pSRski-1, a 1.2-kb *Sst*I fragment from v-*ski*1 [Fig. 2] cloned into pSA801 [26]) (lower panel). Lane M, Molecular weight standards of *Hin*dIII-digested lambda phage DNA detected as described in the legend to Fig. 1 (26).

lyzed by immunoprecipitation with an anti-*gag* serum followed by SDS-PAGE and fluorography (Fig. 5). All of the transfected cells as well as the control SKV-infected cells synthesized both the *gag* precursor protein, $Pr76^{gag}$, and the *pol* precursor protein, $Pr180^{gag\text{-}pol}$. The cells transfected with RAV-SKV5 synthesized an additional protein, p110, which was identical in size both to the major SKV-specific protein synthesized in SKV770-infected cells and to the protein product of SKV780 B12 (Fig. 5).

To examine the structure of the RAV-SKV5 provirus, genomic DNA was prepared from transformed CECs (line 0, ev^-) that had been mass infected with virus from the transfected cells. The genomic DNAs from these cells and from cells infected with a biologically cloned 5.7-kb SKV, SKV785.7 E1, were digested with a set of restriction enzymes and analyzed by Southern blotting and hybridization with a *gag*-specific probe (Fig. 6). The use of line 0 (ev^-) CECs eliminated hybridization to fragments from endogenous viral loci, and the use of a *gag* probe (rather than *ski*) avoided interference by fragments of c-*ski*, allowing us to detect exclusively proviral DNA fragments. The restriction enzymes used distinguish the *env* and long terminal repeat of RAV-1 from homologous regions of tdB77 (Fig. 6a), allowing us to determine whether the virus resulting from transfection with RAV-SKV DNA was the product of that construction or a contaminant derived from one of the natural SKVs. We found that all of the fragments predicted from the maps of RAV-SKV and SKV785.7 (Fig. 6b and c) were detected in the DNAs of infected cells and that the fragments derived from RAV-SKV proviruses were clearly different from those derived from SKV785.7 DNA (Fig. 6d, asterisks).

The digests also contained fragments (Fig. 6d, solid ar-

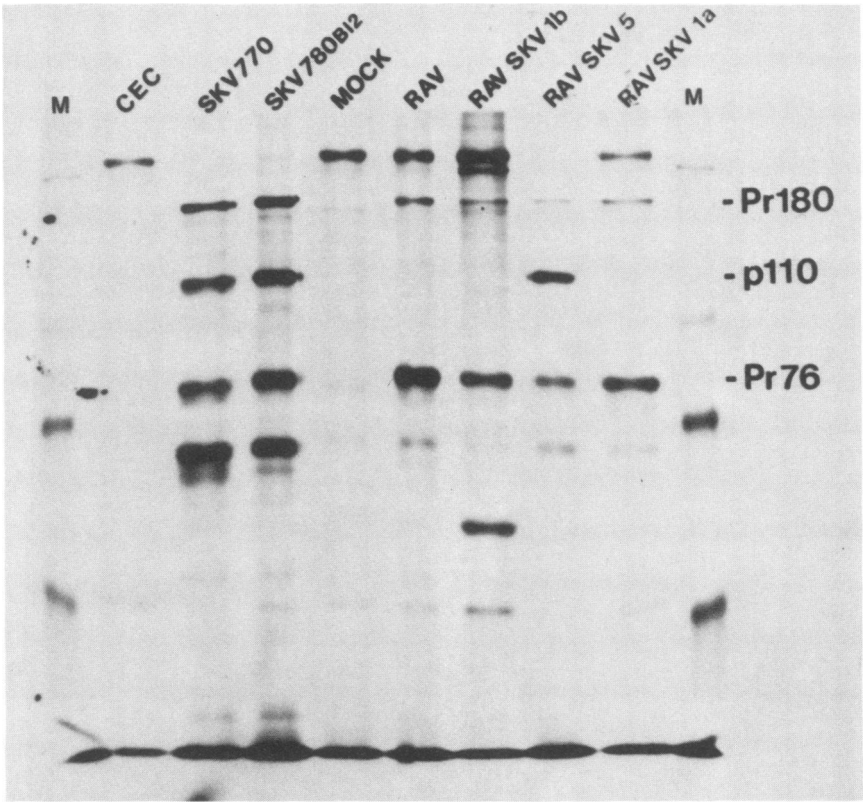

FIG. 5. Immunoprecipitation and SDS-PAGE analysis of viral proteins synthesized in CECs transfected with RAV-SKV DNAs. Transfected and virus-infected CECs as in Fig. 4 were pulse-labeled with [^{35}S]methionine (200 μCi/ml) for 2 h. Labeled viral proteins were analyzed by immunoprecipitation with a *gag*-specific antiserum followed by SDS-PAGE (7.5% polyacrylamide) and fluorography as described in Materials and Methods. Lane M, Protein molecular weight standards: β-galactosidase (92 kilodaltons); bovine serum albumin (66 kilodaltons); ovalbumin (43 kilodaltons).

rows) predicted from the restriction maps of the helper viruses (RAV-1 or tdB77). Additional fragments (i.e., not accounted for by either the 5.7-kb RAV-SKV or RAV-1) were detected in the DNA from RAV-SKV-infected cells (Fig. 6d, open arrows); the likely origin of these fragments was the provirus encoding the 8.9-kb RNA that was detected in these cells as described below.

Generation of 8.9-kb SKV genome from 5.7-kb RAV-SKV. To demonstrate that the RAV-SKV genome alone is capable of inducing transformation, we used the virus harvested from the mass-infected cultures to generate RAV-SKV-transformed nonproducer clones. Both CECs and QECs were infected with this RAV-SKV stock at low multiplicity and cloned either in soft agar or in microtiter wells. Several clones of transformed cells were obtained, some of which were judged to be nonproducers by the absence of pelletable reverse transcriptase in their culture media (data not shown). To verify their producer or nonproducer status, we analyzed intracellular viral proteins. Labeled lysates from several clones, from CECs infected with RAV-1, SKV770, or RAV-SKV produced by the transfected cultures, and from uninfected CECs were analyzed by anti-*gag* immunoprecipitation and SDS-PAGE. The results (Fig. 7) supported the reverse transcriptase data by showing that the three nonproducer clones (19, 23, and 9) contained no Pr76^{gag} although this protein was readily detected in both the virus-producing clones 25 and 7 and in the mass-infected cells. Both producer clones and two of the nonproducer clones synthesized the SKV protein, p110, as expected from the previous analysis of RAV-SKV-transfected cells (Fig. 5). Surprisingly, two samples derived from RAV-SKV-infected cells (the mass-infected culture and clone 9) contained a 125-kilodalton (kDa) protein, p125. In the mass-infected cells p125 was seen in addition to the helper proteins and p110, whereas p125 was the only viral protein detected in the nonproducer clone 9. We had previously identified a p125 protein in SKV770-infected cells (26). That protein (Fig. 7, SKV770 lane) appeared to be identical in size to the RAV-SKV and clone 9 species.

The viral RNAs of both the nonproducer clones and the mass-infected cells were analyzed by Northern blotting cytoplasmic poly(A)-containing RNAs and hybridizing the blot with both *ski* and ALV probes (Fig. 8). The results showed that the p110-containing nonproducer clone 19 contained a single 5.7-kb *ski*-containing genome. This was the genome size of RAV-SKV DNA (Fig. 3) and of the viral RNA from RAV-SKV5-transfected cells (Fig. 4) which also synthesized a p110 (Fig. 5). The p125-synthesizing clone 9 was found to possess a major *ski*-containing RNA of 8.9 kb and three minor RNAs of smaller size. The mass-RAV-SKV-infected cells contained both a 5.7- and an 8.9-kb RNA, while SKV770-infected cells contained these species in addition to other SKV genomes (Fig. 8). Thus, the 8.9-kb virus was not generated during the isolation of clone 9 since both it and its gene product, p125, were detected in the mass-infected population. The fact that the natural SKVs contain a virus with a genome of identical size and encode a p125 protein suggested that analysis of the RAV-SKV-

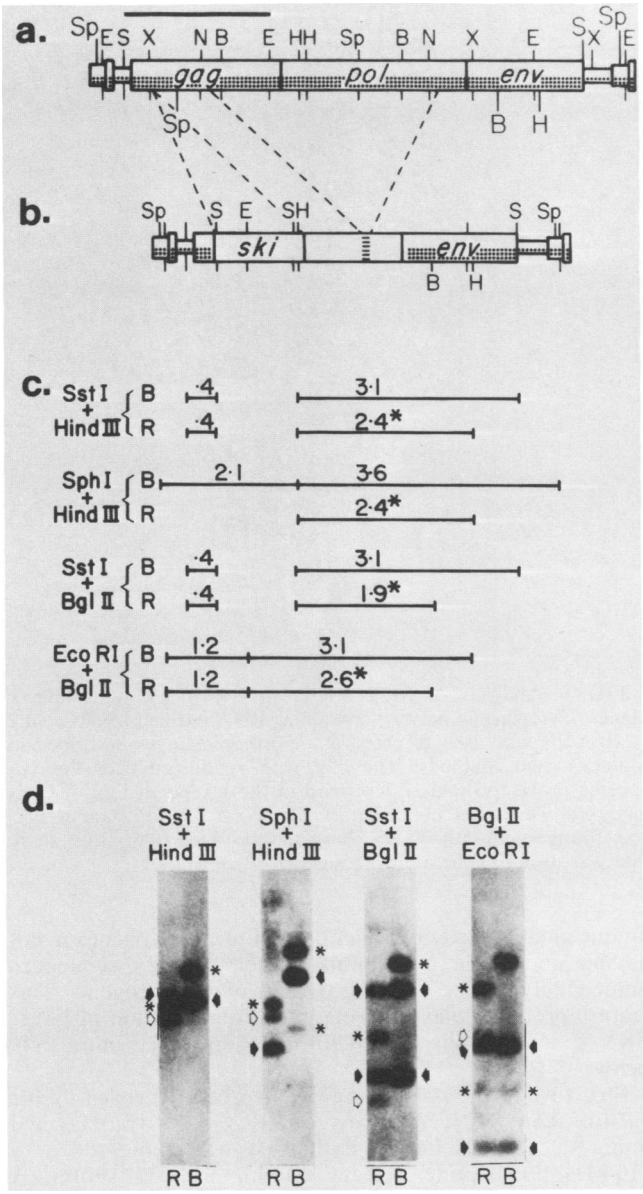

FIG. 6. Southern analysis of DNA from cells infected with RAV-SKV5. Virus harvested from RAV-SKV5-transfected and transformed cells was used to infect fresh CECs prepared from ev$^-$ embryos. These cells were subcultured four times to allow virus spread; at this time all cells appeared transformed. Genomic DNA was purified from these cells, subjected to double restriction enzyme digestions as indicated in the figure, and analyzed by the Southern blotting technique as described in Materials and Methods. The probe used (pB5gag) is the *Sst*I to *Eco*RI fragment indicated by the solid bar above the map in part a. (a) Structural and restriction maps of the genomes of tdB77 (31) (sites above the open structural map) and RAV-1 (sites below the stippled structural map). The *Sph*I (Sp) and *Sst*I (S) sites raised above the other sites in tdB77 are not present in the RAV-1 genome. The *Sph*I, *Bgl*II (B), and *Hin*dIII (H) sites below in the RAV-1 map are not present in the tdB77 genome. Enzymes sites indicated: B, *Bgl*II; E, *Eco*RI; H, *Hin*dIII; N, *Nru*I; S, *Sst*I; Sp, *Sph*I; and X, *Xho*I. (b) Structural and restriction maps of 5.7-kb natural SKV (SKV785.7 E1) shown above the structural map, and the predicted restriction map of RAV-SKV shown below the structural maps. The location of restriction sites for those enzymes used in this experiment are given. As in part a the stippled portion indicates sequences of RAV-1 origin. (c) Fragments predicted from the restriction maps shown in part b that will be detected by the *gag* probe for each double digest indicated. The predicted fragments of SKV785.7 (B) and RAV-SKV (R). Those fragments detected in the analysis of DNA from RAV-SKV5-infected cells that distinguish between the natural and constructed genomes are indicated by an asterisk. (d) Southern blot of DNAs from RAV-SKV (RAV-1)-infected cells (R) and SKV785.7 E1 (tdB77)-infected cells (B). Fragments predicted from the restriction maps of the helper viruses (RAV-1 in the R lanes and tdB77 in the B lanes) are indicated by the solid arrows. Fragments predicted from the maps of the SKV genomes (RAV-SKV in the R lanes and SKV785.7 E1 in the B lanes) are indicated by the asterisks. The additional fragments found only in the R lanes (open arrows) are not predicted from the maps in parts a and b and are discussed in the text. Fragment sizes were determined with *Hin*dIII-digested lambda phage DNA as in Fig. 1.

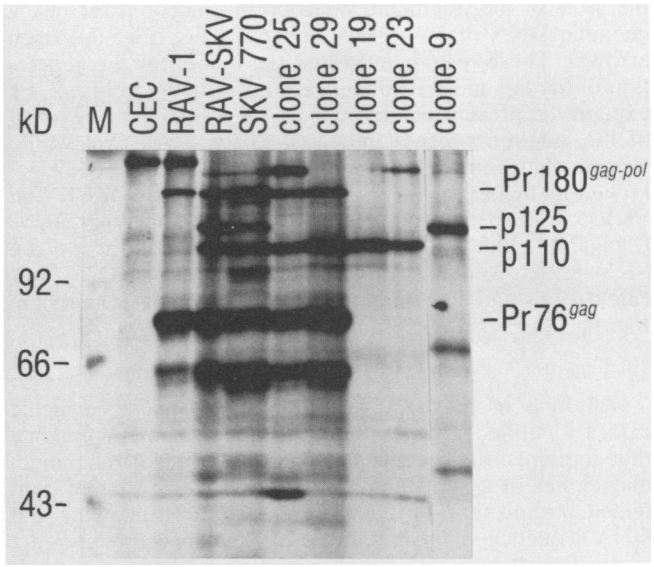

FIG. 7. Viral proteins synthesized in clones transformed by virus harvested from RAV-SKV-infected CECs. Virus harvested from RAV-SKV5-infected cells was used to infect fresh CEC or QEC cultures at low multiplicity of infection (about 0.1 focus-forming unit per cell). After 72 h the infected cells were cloned in agar suspension or in microtiter wells. Transformed clones were grown up in mass culture, and culture fluids harvested from these cultures were assayed for pelletable reverse transcriptase activity. Single culture dishes containing two virus-producer clones (numbers 29 and 25), three nonproducer clones (numbers 9, 19, and 23), SKV770-infected CECs, RAV-1-infected CECs, RAV-SKV5-infected CECs (virus was the same as used to generate transformed clones), and uninfected CECs were labeled with [^{35}S]methionine and analyzed for viral proteins by immunoprecipitation and SDS-PAGE as described in the legend to Fig. 5. kD, Kilodaltons.

derived 8.9-kb virus would be relevant to the persistence of this genome in the natural SKVs.

Having discovered that the 8.9-kb SKV genome and its product p125 were present in the mass-infected CECs we analyzed by Southern blotting, we reexamined the Southern blot of genomic DNA from these cells, focusing on the fragments that were not predicted by the maps of either RAV-SKV or RAV-1 (Fig. 6d, open arrows). Since 8.9 kb is the addition product of RAV-1 (7.6 kb) and *ski* (1.3 kb), we calculated the sizes of fragments predicted if the deletion of *gag* and *pol* sequences in the 5.7-kb genome was restored in the 8.9-kb SKV. The sizes of *gag*-containing fragments predicted by these calculations corresponded exactly with

the sizes of the fragments we could not account for in the genomic DNA of RAV-SKV-infected cells (Fig. 6d, open arrows). These results suggested the model for the generation of the 8.9 and 5.7-kb natural SKVs shown in Fig. 9. To explain the present results, which are essentially a reversal of the deletion process indicated in the figure, we would suggest that homologous recombination between SKV 5.7 kb and its helper virus (in the stippled regions of tdB77 and SKV 5.7 kb in the figure) would produce an 8.9-kb SKV. Cleavage at the *Bgl*II and *Hin*dIII sites shown above the SKV 8.9-kb genome yields fragments predicted by our calculations and detected in the Southern analysis shown in Fig. 6d.

DISCUSSION

Definition of the SKV oncogene, *ski*. An SKV-specific cDNA identified a single region of the 5.7-kb SKV genome that contained the specific sequence *ski*. We isolated molecular clones of a subgenomic restriction fragment that contained *ski* and found by combined restriction mapping and DNA sequence analysis that the *ski* sequence constituted a single insertion of 1.3 kb of cell-derived DNA sequence bounded by *gag* gene sequences of the helper virus, tdB77. When we inserted this restriction fragment bearing *ski* and 1.5 kb of flanking helper virus sequence into an appropriately deleted helper virus genome, a biologically active SKV was generated. Chicken cells infected with this virus, RAV-SKV, formed typical SKV foci in monolayer cultures and produced colonies in soft agar. Low-multiplicity infection with RAV-SKV yielded colonies of transformed nonproducer cells, showing that the SKV genome alone is capable of transforming avian cells. Since the 1.3-kb *ski* sequence was the only information in RAV-SKV that was not derived from the nontransforming viruses tdB77 and RAV-1 and since *ski* constituted the only SKV-specific sequence that was held in common by all of the SKV genomes (16), it followed that *ski* was the only oncogene of SKVs.

Structure of the 5.7-kb SKV genome. We constructed a physical map of the major provirus (5.7 kb) in SKV770-infected cells by hybridizing Southern blots with probes for both ALV and *ski*. This map indicated that *ski* occupied the site of a large deletion of *gag* and *pol* sequences in a genome which otherwise corresponded to the SKV helper virus, tdB77. However, our subsequent analysis of molecular clones derived from the 5.7-kb provirus revealed that the site of *ski* insertion in the p19 region of the *gag* gene was 0.7 to 1.0 kb upstream from the 5′ end of the deletion. These findings suggested that the recombination events which generated SKV did not result in the deletion of any tdB77 sequences. In that case we would propose that the original SKV would have been 8.9 kb (a 1.3-kb *ski* insertion into the 7.6-kb tdB77 genome), and a viral RNA of approximately that size was present in all of the natural SKV isolates (26). The other SKV genomes would then have arisen subsequently by deletion of helper virus sequences.

Our sequence data suggested a possible mechanism for the generation of a nondeleted *ski*-containing genome. We found that *ski* was flanked by a direct repeat of a hexanucleotide which was present only once at that site in two viruses closely related to tdB77 (24, 27). This configuration resembles the repeats of target sequences generated by insertion of transposable elements (6, 28, 30). However, the *ski* sequences immediately inside the repeats did not constitute either direct or inverted repeats as expected if *ski* had inserted into tdB77 by transposition (6, 28, 30). Whatever the mechanism for generating SKV, its genome structure is unique among retroviruses with *gag*-linked oncogenes in not having undergone a deletion of helper virus sequences immediately adjacent to the 3′ end of its oncogene. This feature probably played a role in the regeneration of larger SKV genomes from deleted forms as discussed more fully below.

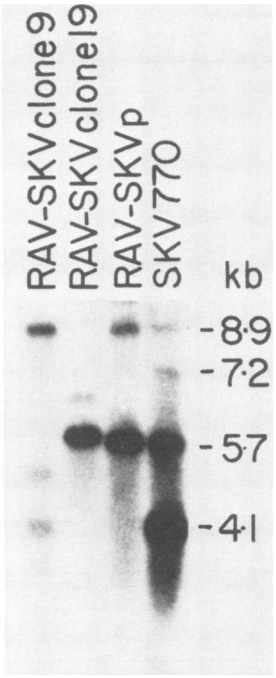

FIG. 8. Analysis of SKV RNAs in RAV-SKV nonproducer clones. Cytoplasmic poly(A)-containing RNA purified from about 2×10^6 cells was used to prepare a Northern blot as described in Materials and Methods. The blot was hybridized with the *ski*-specific probe (pSRski-1) described in the legend to Fig. 4. Cells analyzed were two nonproducer clones, 9 and 19, and CECs transformed with either SKV770 or the passaged RAV-SKV stock that was used to generate the transformed clones.

Structure of the *ski*-containing polyprotein encoded by the 5.7-kb RAV-SKV. Analysis of RAV-SKV-transformed nonproducer cells indicated that *ski* was expressed as a 110-kDa polypeptide detectable with anti-*gag* serum. A protein of identical size was shown to be the major species encoded by the natural SKVs, and analysis of the p110 encoded by SKV770 with several monospecific antisera showed that it contained antigenic determinants of the *pol* gene and the *gag* genes p19 and p27 but not of the *gag* genes p12 and p15 nor of the *env* gene (26). Our present mapping and sequence data predicted that a protein of exactly 110 kDa would result from translation of the sequence of the RAV-SKV genome extending from the *gag* initiation codon to the *pol* termination codon. This polypeptide would have the form N terminus-p19-*ski*-p19-p10-p27*-**pol*-C terminus; the carboxy-terminal half of p27, all of p12 and p15, as well as the amino terminal 80% of *pol* were included in the large deletion which produced the 5.7-kb SKV. Thus, in both size and structure the polypeptide predicted from our analysis of the cloned SKV DNA conformed to the proteins encoded by RAV-SKV and SKV770.

We had previously suggested that the 5.7-kb genome encoded p125 because we failed to detect *pol* sequences in this genome by Northern blot analysis and p125 was shown to contain antigenic determinants of *gag* but not of *pol* (26).

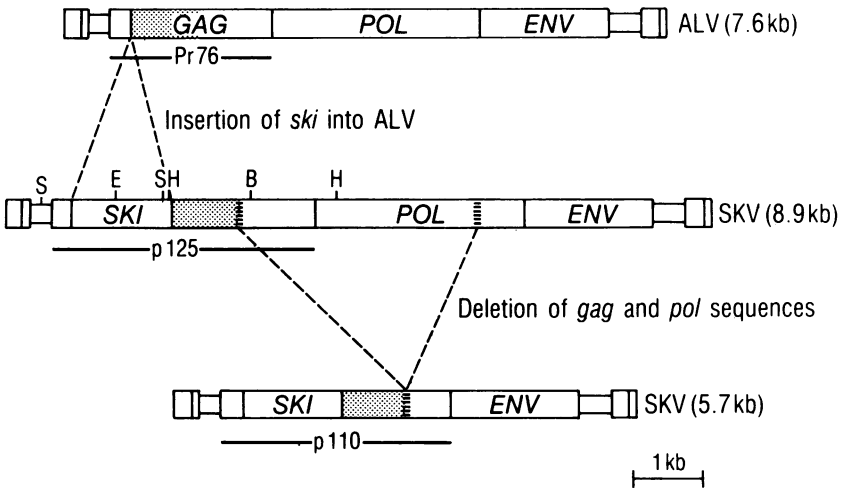

FIG. 9. Model for the generation of 8.9-kb and 5.7-kb SKV genomes. The figure shows the genetic and partial restriction maps of tdB77 and SKV 5.7 kb as well as the proposed map of the 8.9-kb genome. The sites for *Bgl*II (B) in *gag* and for *Hin*dIII in *pol* shown above the SKV (8.9-kb) genome support this model since they are known sites in tdB77 and are consistent with fragments detected in DNA from RAV-SKV5-infected cells (Fig. 6). The model proposes that the initial SKV was the undeleted 8.9-kb form in which *ski* is inserted in the p19 *gag* gene. This virus encodes the *gag-ski-gag* p125 protein indicated by the dark bar below the genome. Subsequently, a 3.2-kb deletion of the sequence indicated gave rise to the 5.7-kb SKV genome that encodes the *gag-ski-gag-pol* p110 protein. To regenerate the 8.9-kb SKV genome from the 5.7-kb form requires only a single recombination between the 5.7-kb SKV and tdB77 (or any helper virus) in the region of the *gag* gene indicated by stippling.

We have repeated the Northern analysis using separate probes representing either the 5′ or 3′ half of the *pol* gene and find that the 5.7-kb genome hybridizes only with the 3′ *pol* probe (data not shown). This result confirms our present analysis and suggests that our previous failure to detect these sequences derived from the use of a 2.7-kb probe to detect about 200 bases of *pol*-derived sequence.

The helper-derived sequences on the 3′ side of *ski* in the 5.7-kb SKV preserved their translational reading frame despite two recombination events. Originally it seemed so unlikely that this would have occurred and persisted by chance that we felt these sequences must play a role in the transformation function of the polypeptide. We now know that the p125 encoded by the 8.9-kb SKV is also a transforming protein although its carboxy-terminal third is completely different from that of p110 (26). Furthermore, we have recently isolated transforming SKVs which encode proteins that do not appear to contain any helper-derived polypeptide on the C-terminal side of *ski* (unpublished data). These findings have led us to believe that either there was no biological significance ascribable to the preservation of the reading frame in the *gag-pol* region of p110 or that its significance was incidental to translation but reflected sequence requirements for the two recombination events. If this was the case we might expect these requirements to be revealed by analyzing the sequences of both the c-*ski-gag* recombination sites and the deletion boundaries in *gag* and *pol*.

Generation of an 8.9-kb SKV genome from a 5.7-kb form. Studies with several retroviruses, most notably RSV (7, 11) and Abelson murine leukemia virus (13), demonstrated that deletion of sequences that were not essential for transformation or viral replication occurred at a relatively high frequency. In RSV stocks deletion of the *src* gene resulted in the accummulation of transformation-defective variants which eventually became the predominant form in multiply passaged stocks of the virus. With Abelson murine leukemia virus, deletion of the 3′ half of the *abl* gene progressed until a minimum transforming gene (encoding a 90-kDa protein compared with the original 160-kDa protein) remained (13). With these examples in mind it was not surprising to find multiple forms of *ski*-containing genomes in our SKV stocks, particularly when we considered it likely that SKVs had not been passaged long enough for one of the forms to predominate (26). However, contrary to the prediction of an ongoing process of deletion, we observed that the relative amount of the largest genome (8.9 kb) in our frequently passaged stocks of SKV770 did not decrease with virus passage. This apparent contradiction was resolved by the results presented in the present study which showed that a molecularly cloned 5.7-kb SKV genome could generate an 8.9-kb genome upon transfection and subsequent virus spread.

It appears that the 8.9-kb SKV arose from the 5.7-kb genome by a simple recombination which essentially reversed the deletion of *gag* and *pol* sequences that presumably generated the 5.7-kb genome from the 8.9-kb form (this model is shown in Fig. 9). This conclusion derives from both our Southern blot analysis (Fig. 6) and our present and previous analyses of p125, the protein encoded by the 8.9-kb SKV. Our structural analysis of the genome indicates that *gag* sequences deleted from the 5.7-kb genome were restored in generating the 8.9-kb form. Translation of this genome from the normal *gag* initiator should then yield a polypeptide that terminates at the end of the *gag* gene. This protein would have the form N terminus-p19-*ski*-p19-p10-p27-p12-p15-C terminus and its size would be the addition product of *ski* (49 kDa) and *gag* (76 kDa) or a total of 125 kDa. We had previously described a p125 of SKV770 that contained p19, p27, p12, and p15 antigenic determinants (we didn't have anti-p10 antiserum) but did not contain determinants of either *pol* or *env* (26). In the present study we described a nonproducer clone transformed by an 8.9-kb SKV that synthesized only one *gag*-containing protein, p125. The agreement between the present results and the previous analysis of the natural SKVs suggests that the 8.9-kb genome generated from RAV-SKV is identical in

sequence organization to the 8.9-kb genome in SKV770. We recently isolated a producer clone of SKV770-transformed cells that contained only an 8.9-kb SKV genome and synthesized only p125; Southern analysis of the provirus in the clone produced results that are totally consistent with the structure we proposed for the 8.9-kb RAV-SKV in Fig. 9 (J. Teumer, D. Brodeur, and E. Stavnezer, unpublished data). Therefore, we would suggest that the events which generated the 8.9-kb genome from RAV-SKV provide a model for the observed preservation of the 8.9-kb genome in the natural isolates despite an ongoing process of helper sequence deletion.

The simplest model to explain the generation of the 8.9-kb genome in the present study invokes a single homologous recombination between the 5.7-kb genome and the RAV-1 genome within the 0.7- to 1-kb segment of *gag* sequence that lies between the 3′ end of *ski* and the deletion site in the 5.7-kb genome (Fig. 9, stippled regions of tdB77 and SKV 5.7 kb). This ability to repair helper sequence deletions is an unusual feature of SKV and probably derives from the facts that the acquisition of *ski* did not involve deletion of helper sequences and that subsequent deletions occurred at sites somewhat removed from the *ski* insertion site. All other defective transforming viruses bear sizable helper sequence deletions at the site of oncogene insertion; homologous recombination between these viruses and their helpers would have only regenerated the sequence organization of the two starting genomes.

The rapidity with which the 8.9-kb genome appeared in our RAV-SKV stock was consistent with the high frequency of recombination that had been observed between related avian retroviruses (7, 15). Two models advanced to explain the high recombination frequency invoked copackaging of the two starting genomes in a single virus particle followed by recombination either during (7) or following (15) the synthesis of viral DNA in an infected cell. While either of these mechanisms could underlie the present results, we must also consider the likely possibility that recombination could have occurred between the two transfected viral genomes within the transfected cells. Homologous recombination of this type has been shown to occur at a relatively high frequency (2, 17). Regardless of whether the present results involved recombination during transfection or virus spread, they suggest a plausible model for the regeneration of larger SKV genomes from smaller forms.

ACKNOWLEDGMENT

This work was supported by grants from the National Cancer Institute (CA 32817 and CA 08748).

LITERATURE CITED

1. **Astrin, S. M., H. L. Robinson, L. B. Crittenden, E. G. Buss, J. Wyban, and W. S. Hayward.** 1980. Ten genetic loci in the chicken that contain structural genes for endogenous avian leukosis viruses. Cold Spring Harbor Symp. Quant. Biol. **44**:1105–1109.
2. **Bandyopadhyay, P. K., S. Watanabe, and H. M. Temin.** 1984. Recombination of transfected DNAs in vertebrate cells in culture. Proc. Natl. Acad. Sci. USA **81**:3476–3480.
3. **Benton, W. D., and R. W. Davies.** 1977. Screening lambda gt recombinant clones by hybridization to single plaques in situ. Science **196**:180–192.
4. **Bishop, J. M.** 1983. Cellular oncogenes and retroviruses. Annu. Rev. Biochem. **52**:301–354.
5. **Bishop, J. M., and H. E. Varmus.** 1982. Functions and origins of retroviral transforming genes, p. 999–1108. *In* R. Weiss, N. Teich, H. Varmus, and J. Coffin (ed.), Molecular biology of tumor viruses, part III: RNA tumor viruses. Cold Spring Harbor Laboratory, Cold Spring Harbor, N.Y.
6. **Calos, M. P., and J. H. Miller.** 1980. Transposable elements. Cell **20**:579–595.
7. **Coffin, J. M.** 1979. Structure, replication, and recombination of retrovirus genomes: some unifying hypotheses. J. Gen. Virol. **42**:1–26.
8. **Corsaro, C. M., and M. L. Pearson.** 1981. Enhancing the efficiency of DNA mediated gene transfer in mammalian cells. Somatic Cell Genet. **7**:603–616.
9. **DeLorbe, W. J., P. A. Luciw, H. M. Goodman, H. E. Varmus, and J. M. Bishop.** 1980. Molecular cloning and characterization of avian sarcoma virus circular DNA molecules. J. Virol. **36**:50–61.
10. **Denhardt, D. T.** 1966. A membrane-filter technique for the detection of complementary DNA. Bicohem. Biophys. Res. Commun. **23**:641–646.
11. **Fincham, V. J., P. E. Neiman, and J. A. Wyke.** 1980. Novel nonconditional mutants in the *src* gene of Rous sarcoma virus: isolation and preliminary characterization. Virology **103**:99–111.
12. **Fleissner, E.** 1970. Virus-specific antigens in hamster cells transformed by Rous sarcoma virus. J. Virol. **5**:14–21.
13. **Goff, S. F., O. N. Witte, E. Giboa, N. Rosenberg, and D. Baltimore.** 1981. Genome structure of Abelson murine leukemia virus variants: proviruses in fibroblasts and lymphoid cells. J. Virol. **38**:460–468.
14. **Hughes, S. H., P. R. Shank, D. H. Spector, H.-J. Kung, J. M. Bishop, and H. E. Varmus.** 1978. Proviruses of avian sarcoma virus are terminally redundant, co-extensive with unintegrated linear DNA and integrated at many sites. Cell **15**:1397–1410.
15. **Hunter, E.** 1978. The mechanism for genetic recombination in the avian retroviruses. Curr. Top. Microbiol. Immunol. **79**:295–309.
16. **Li, Y., C. M. Turck, J. K. Teumer, and E. Stavnezer.** 1986. Unique sequence, *ski*, in Sloan-Kettering avian retroviruses with properties of a new cell-derived oncogene. J. Virol. **57**:1065–1072.
17. **Lin, F.-L., K. Sperle, and N. Sternberg.** 1984. Model for homologous recombiation during transfer of DNA into mouse L cells: role for DNA ends in the recombination process. Mol. Cell. Biol. **4**:1020–1034.
18. **Loenen, W. A. M., and W. J. Brammar.** 1980. A bacteriophage lambda vector for cloning large DNA fragments made with several restriction enzymes. Gene **20**:249–259.
19. **Maniatis, T., E. F. Fritsch, and J. Sambrook.** 1982. Molecular cloning, a laboratory manual. Cold Spring Harbor Laboratory, Cold Spring Harbor, N.Y.
20. **Maxam, A. M., and W. Gilbert.** 1980. Sequencing end-labeled DNA with base-specific chemical cleavages. Methods Enzymol. **65**:499–560.
21. **McMaster, G., and G. Carmichael.** 1977. Analysis of single-stranded and double-stranded nucleic acids on acrylamide and agarose gels with glyoxal and acridine orange. Proc. Natl. Acad. Sci. USA **74**:4835–4838.
22. **Purrello, M., and I. Balazs.** 1983. Direct hybridization of labelled DNA to DNA in agarose gels. Anal. Biochem. **128**:393–397.
23. **Rigby, P. W., M. Dieckmann, C. Rhodes, and P. Berg.** 1977. Labeling deoxyribonucleic acid to high specific activity in vitro by nick translation with DNA polymerase I. J. Mol. Biol. **113**:237–251.
24. **Schwartz, D. E., R. Tizard, and W. Gilbert.** 1983. Nucleotide sequence of Rous sarcoma virus. Cell **32**:853–869.
25. **Southern, E. M.** 1975. Detection of specific sequences among DNA fragments separated by gel electrophoresis. J. Mol. Biol. **98**:503–517.
26. **Stavnezer, E., D. S. Gerhard, R. C. Binari, and I. Balazs.** 1981. Generation of transforming viruses in cultures of chicken fibroblasts infected with an avian leukosis virus. J. Virol. **39**:920–934.
27. **Swanstrom, R., H. E. Varmus, and J. M. Bishop.** 1982. Nucleotide sequence of the 5′ noncoding region and part of the *gag*

gene of Rous sarcoma virus. J. Virol. **41**:535–541.
28. **Temin, H. M.** 1980. Origin of retroviruses from cellular movable genetic elements. Cell **21**:599–600.
29. **Thomas, P. S.** 1980. Hybridization of denatured RNA and small DNA fragments transferred to nitrocellulose. Proc. Natl. Acad. Sci. USA **77**:5201–5205.
30. **Varmus, H. E.** 1982. Form and function of retroviral proviruses. Science **216**:812–820.
31. **Varmus, H. E., N. Quintrell, and S. Ortiz.** 1981. Retroviruses as mutagens: insertion and excision of a nontransforming provirus alter expression of a resident transforming provirus. Cell **25**:23–36.
32. **Weiss, S. R., H. E. Varmus, and J. M. Bishop.** 1977. The size and genetic composition of virus-specific RNAs in the cytoplasm of cells producing avian sarcoma-leukosis viruses. Cell **12**:983–992.